Tracking lineages of single cells in lines using a microfluidic device

Amy C. Rowat[a,1], James C. Bird[a], Jeremy J. Agresti[a], Oliver J. Rando[b], and David A. Weitz[a,1]

[a]Department of Physics/School of Engineering and Applied Sciences, Harvard University, Cambridge, MA 02138 ; and [b]Department of Biochemistry and Molecular Pharmacology, University of Massachusetts Medical School, Worcester, MA 01605

Cells within a genetically identical population exhibit phenotypic variation that in some cases can persist across multiple generations. However, information about the temporal variation and familial dependence of protein levels remains hidden when studying the population as an ensemble. To correlate phenotypes with the age and genealogy of single cells over time, we developed a microfluidic device that enables us to track multiple lineages in parallel by trapping single cells and constraining them to grow in lines for as many as 8 divisions. To illustrate the utility of this method, we investigate lineages of cells expressing one of 3 naturally regulated proteins, each with a different representative expression behavior. Within lineages deriving from single cells, we observe genealogically related clusters of cells with similar phenotype; cluster sizes vary markedly among the 3 proteins, suggesting that the time scale of phenotypic persistence is protein-specific. Growing lines of cells also allows us to dynamically track temporal fluctuations in protein levels at the same time as pedigree relationships among the cells as they divide in the chambers. We observe bursts in expression levels of the heat shock protein Hsp12-GFP that occur simultaneously in mother and daughter cells. In contrast, the ribosomal protein Rps8b-GFP shows relatively constant levels of expression over time. This method is an essential step toward understanding the time scales of phenotypic variation and correlations in phenotype among single cells within a population.

epigenetics | protein expression | single cell assay | yeast

Nearly 150 years ago, Mendel elucidated the fundamental unit of heredity by tracing and applying statistics to inheritance patterns in pea plants. In most cases, heritable phenotypic variation arises from differences in DNA sequence, yet even cells that are genetically identical can exhibit distinct, heritable states that are critical during differentiation and development, and possibly in response to environmental stress. Phenotypic variation that occurs on time scales shorter than the characteristic cell division time is known to result from the stochastic processes inherent to gene and protein expression (1). However, variations in protein levels at frequencies longer than the typical generation time enable phenotypic states to be passed on to genetically identical progeny cells, a phenomenon known as epigenetic inheritance (1, 2); the time scales of such multigenerational variation are less well understood. Mechanisms that generate phenotypic variation that propagates over many cell divisions include positive feedback loops in genetic networks (3–5), protein aggregation (6), and chromatin state (2, 7). Phenotypic variation may provide a fitness advantage for a population of cells in a fluctuating environment (8), and the ability to inherit phenotype is proposed to benefit populations in conditions in which the environment changes on time scales faster than genetic mutations occur (9). Such bet-hedging in microbial populations may have medical consequences: for example, a subset of "persistor" cells within an actively growing population of bacteria divides more slowly and shows increased antibiotic resistance (10). Despite the importance of epigenetic mechanisms of gene regulation, the time scales of variation at the single cell level remain poorly understood.

To study the phenotype of single cells in the context of pedigree demands a method to collect data over many cells and over many generations. The budding yeast, *Saccharomyces cerevisiae*, is a good model eukaryotic system: yeast cells divide rapidly, making it technically feasible to study multiple generations of cells. Proteome-wide studies of *S. cerevisiae* have characterized stationary distributions of protein levels across a population by microscopy and flow cytometry, revealing that expression of stress-related genes tends to be more variable ("noisy"), whereas housekeeping genes exhibit less cell-to-cell variation (11–14). However, these measurements capture neither changes in expression over time nor correlations in protein levels resulting from age or pedigree relationships among individuals. To characterize cells and their progeny requires following single cells and their offspring during growth; this can be achieved by individually separating cells by micromanipulation (15) or by imaging cells as they grow sandwiched between an agar pad and a cover glass (5). However, manual manipulation of cells is laborious, and accurately determining pedigree and protein expression by microscopy is challenging as cells grow out of the focal plane after only a few divisions. Various microfluidic devices maintain cells in a single focal plane as they grow (10, 16–21), but many of these devices require sophisticated fabrication techniques such as multilayer fabrication with valves (16, 18), channel height differences (17), or membranes (10, 21). To optimize the statistical power of these techniques, the initial placement of cells should be controlled; several other microfluidic devices achieve single-cell trapping (22–24), but these trapping mechanisms are not conducive to the lineage analysis that we perform here. The ability to robustly and repeatedly trap, spatially organize, and track the growth of single cells over many generations in a device that is easy to fabricate and simple to use would enable the collection of data over many cell lineages in a single experiment.

Here we introduce a simple microfluidic device for following lineages deriving from single yeast cells. We seed single parental cells into channels fabricated at a high density to maximize the number of lineages tracked in each experiment. To simplify tracking both pedigree and levels of protein expression, we geometrically constrain the cells to divide in a line within a single focal plane. Furthermore, we design the device so that fluid can constantly perfuse through the device, which allows us to replenish media, change environmental conditions, and perform other analyses. For example, we are able to fix and stain the cells in situ. By studying protein expression in the context of pedigree, we are able to see patterns of expression where phenotype is correlated over multiple

CELL BIOLOGY

ENGINEERING
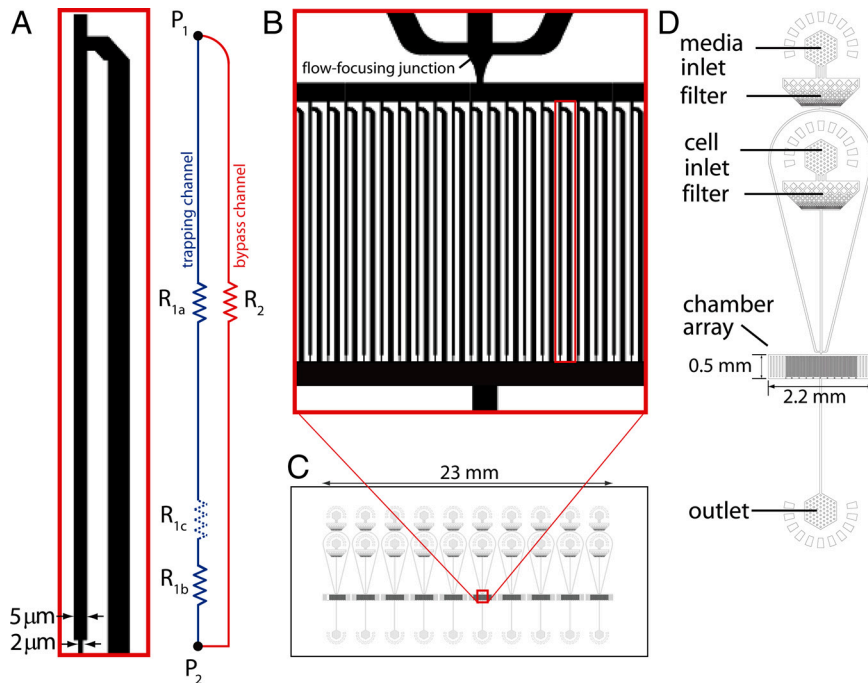
Fig. 1. Lineage chamber device layout. (*A*) A single chamber consists of a long channel with a 5-μm width and a 2-μm constriction, as shown in this inset of *B*. The flow patterns can be understood in terms of an electrical circuit, with R_{1a}, the resistance of the trapping chamber; R_{1b}, the resistance of the constriction; R_{1c}, the resistance of a single cell; and R_2, the resistance of the bypass channel. The pressure drop ($P_1 - P_2$) is equivalent for both fluid paths. (*B*) The chamber array consists of 50 chambers arranged in parallel, approximately half of which are active and shown in this inset of *C*. A flow-focusing geometry centers the flow of the cells into the chamber array. (*C*) Ten individual devices fit onto a 50 × 24-mm coverslip enabling multiple conditions or cell types to be tested in a single experiment. (*D*) Overview of the entire lineage chamber device. Two inlets allow for separate flow paths of the cell suspension and media. Filters eliminate aggregates of cells.

generations; such information remains hidden when studying at the population as an ensemble.

**Device Concept.** To facilitate analysis of single cells and their progeny, we designed a microfluidic device in which lineages deriving from single cells are spatially organized in lines. For nearly a century, linear arrays of spores encapsulated in natural, rod-shaped ascal sacs have proven useful for elucidating the mechanisms of Mendelian inheritance (25); more recently, lineages of bacterial cells in lines have been studied in microfluidic devices (10). However, when placing cells in chambers of a fabricated device, the distribution of cells is random, with the number of cells per chamber dictated by Poisson statistics. To achieve a high proportion of single cells seeded in the linear chambers, we fabricated an array of chambers that have a constriction at one end, so cells are trapped when they flow into the chambers (Fig. 1*A*). After one cell enters a chamber, the ratio of flow through the chamber to bypass channels shifts, increasing the probability that subsequent cells preferentially enter the bypass channel instead of the growth chamber (26). Importantly, our device is easily fabricated by using a single cast of polydimethylsiloxane (PDMS) and requires only a syringe pump and microscope for operation.

To understand the single cell trapping mechanism, we estimate the flow rate through the microfluidic device by using lumped element modeling, an approach often used to analyze simple electrical circuits. The volumetric flow rate, Q, through the channels is analogous to electrical current; the pressure drop, ΔP, is analogous to the voltage drop; and the remaining factors describe the fluidic resistance that depends largely on the channel geometry. The trapping (Fig. 1*A*, blue) and bypass (Fig. 1*A*, red) channels act as 2 lumped resistors in parallel; the pressure drop across both channels must be equal because the end points are the same, $\Delta P_1 = \Delta P_2$ (Fig. 1*A*). For efficient single cell trapping, the presence of a cell in the trapping channel should change the flow such that

subsequent cells do not enter. Thus, when the trapping channel is empty, the flow through the bypass channel, Q_2, should be less than the flow through the trapping channel, Q_1; when a single cell is present in the channel, Q_2 should be greater than Q_1 so that most of the flow, and therefore subsequent cells, flow through the bypass channel (27). We design the device given this criterion and other geometric requirements, as outlined in the *SI Text*. For example, to spatially organize the microcolonies that derive from the array of single cells and force them to grow in a single focal plane, we engineered the growth chambers with a square cross-section that is the width and height of an average single cell, $w_{1a} = h_2 = h_{1a} = 5$ μm.

Given these prerequisites, we designed the device with an array of 50 chambers (Fig. 1*D*); roughly half of these are active chambers that fill with cells (Fig. 1*B*). Because 10 or more devices can be fabricated on each chip (Fig. 1*C*), hundreds of cells can be trapped, enabling the simultaneous testing of different flow conditions or cell types in a single experiment. We loaded cells into the device by activating 2 syringes that contain the cell suspension and growth media (Fig. 1*D* and Fig. S1). To provide greater control between the 2 fluid streams, we fabricated a flow-focusing junction at the entry to the chamber array: the cells flow down the center while the media flows in from the sides (Fig. 1*B*). This geometry prevents cells from flowing into the media line, and thus maintains a cell-free source of media for perfusion during the experiment. When single cells are loaded, we deactivate the cell-loading inlet by disconnecting the tubing from the syringe. To allow for metabolite exchange during cell growth, we continually flow media through the device during the experiment; as the cells are round and the channels are square, media perfuses through the chambers as cells grow. The continued media flow also ensures there is constant flow backward through the cell inlet, preventing cells trapped upstream from entering the chamber array (Fig. S1).
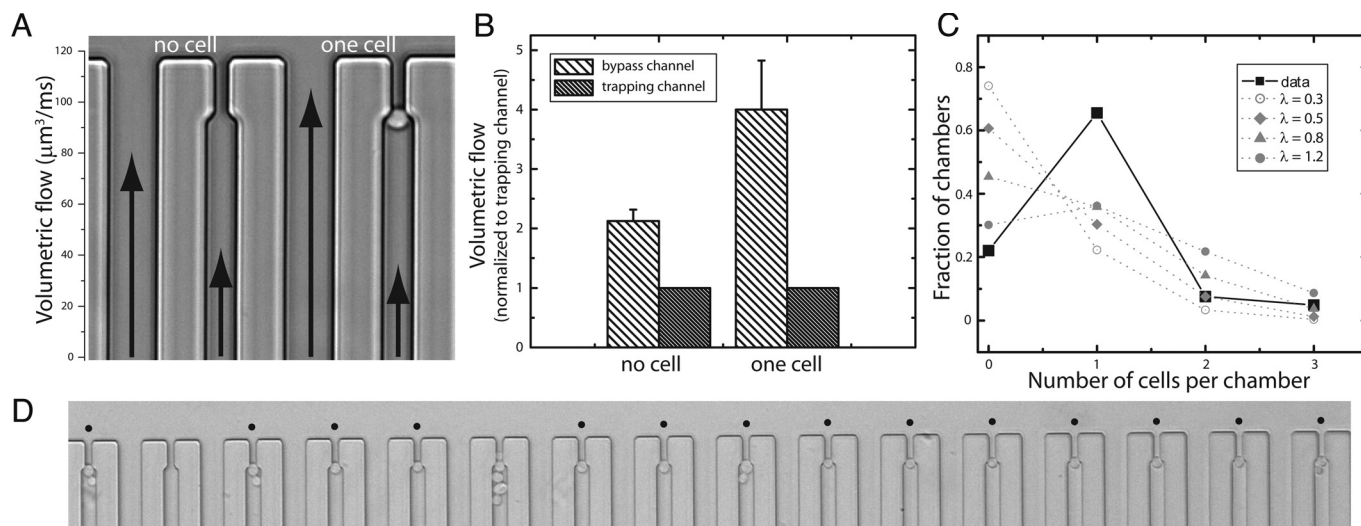
Fig. 2. Trapping single cells in the lineage chambers. (*A*) Average volumetric flow rates through the bypass and trapping channels are proportional to the length of arrows superimposed on this bright-field image. Flow through the bypass channel doubles when a single cell is trapped, increasing the probability for cells to flow through the bypass while still allowing for fluid flow through the trapping channel. (*B*) Volumetric flow through the bypass channel normalized to the trapping channel. Error bars represent SD for $n = 6$ (bypass) and $n = 9$ (trapping) channels. (*C*) After loading, there are 0.8 cells per active chamber. Data shown here are summed over 30 independent experiments. Plotting an equivalent Poisson distribution ($\lambda = 0.8$) would result in less than 40% chambers containing single cells (gray triangles), as well as chambers that are empty or contain multiple cells. Other gray symbols represent Poisson distributions for other λ values. (*D*) Bright-field image showing an array of trapping chambers filled with single cells that are identified by black dots. (Channel width, 5 μm.)

Results and Discussion

To demonstrate our single cell trapping mechanism, we measure the flow through the chamber and bypass channels by imaging tracer particles: when the trapping channel is empty, the volumetric flow through the bypass channel, Q_2, is approximately twice that through the trapping channel, Q_1: $Q_2/Q_1 = 2.1 \pm 0.2$ ($n = 6$; Fig. 2 *A* and *B*). This value is in excellent agreement with simple estimates of flow when the trapping chamber is empty (Eq. **1** and *SI Text*). Thus, while cells are loading, many of them pass through the bypass channel, and some cells flow into the chambers. However, when a single cell is trapped in the lineage chamber channel, the flow through the bypass channel increases to $Q_2/Q_1 = 4.0 \pm 0.8$ ($n = 9$; Fig. 2 *A* and *B*) as a result of the decrease in the cross-sectional area of the trapping channel. The resulting change in fluidic resistance upon trapping a single cell increases the probability that additional cells are diverted through the bypass channel instead of the trapping channel. Importantly, the continued flow even in the presence of a trapped cell allows for media exchange during cell growth.

With this method, device loading is complete within 2 to 3 min with good single cell trapping efficiency: on average, 70% of the active chambers fill with single cells (Fig. 2 *C* and *D*). The majority of the remaining chambers are empty, and some contain multiple cells. If the loading of cells were completely random and independent of the number of previously trapped cells, the number of cells per chamber would follow a Poisson distribution whereby, for the same average number of cells trapped per chamber, the majority of chambers would be empty, only 40% would have single cells, and a smaller number would contain multiple cells (Fig. 2*C*); our loading mechanism thus achieves much better efficiency than dictated by Poisson statistics. Note that deviations from ideal loading with 100% single cells may result from the low flow ratio between bypass and trapping channels (27), variations in cell size, asymmetry in cell shape, or differences in cell stiffness that may affect the extent to which a cell deforms into the constriction and blocks the channel.

As the cells divide in the long, narrow growth chamber, they are constrained to grow in a line. To evaluate growth of cells in the lineage chambers, we acquire images of cells at 10-min intervals (Fig. 3*A*). We compare growth of cells in chambers to those on agar pads, a common method for time-lapse imaging of yeast cells. Analysis of the time between buddings for single cells shows that doubling time is similar for cells cultured in the lineage chambers and on agar pads (Fig. 3*B*). For a given cell, we observe a relatively constant division time over the course of the experiment even for cells at the bottom of the chamber. To determine if media exchange is hindered by an increasing number of cells per chamber, we flow a solution containing fluorescent probe through chambers filled with cells. We observe that all cells along the channel become fluorescently labeled, showing that liquid penetrates around cells along the length of the channel, and confirming that fluid exchange happens on the order of minutes (Fig. S2).

We analyze lineages of cells by using the device in one of 2 ways: in endpoint mode, in which we acquire a single image at the end of the growth experiment, or in kinetic mode, in which we quantitatively track protein levels in single cells over time. To illustrate the utility of the device, we investigate the expression of 3 representative proteins, each with a distinct expression pattern. As an example of endpoint mode, we first study the expression of the protein Pho84, a high-affinity phosphate transporter, whose expression is subject to positive feedback and exhibits bimodal expression when cells are grown in intermediate phosphate concentrations (28). Expression of Pho84 is expected to switch between the "on" and "off" phenotypic states at some frequency; yet from images of cells in bulk acquired at a single time point (Fig. 4*A*), or from the stationary distribution obtained by flow cytometry (Fig. S3) (28), the time of switching between states cannot be determined. To address this question, we image cells expressing pPho84-GFP after growth in the lineage chambers. Each line represents a lineage deriving from a single cell with domains of cells that are closely related genealogically (Fig. 5, gray bars). The frequency of phenotypic variation is easily determined by visually inspecting the lines of cells, and can be quantified with simple image analysis. In some cases, entire lineages of cells have a similar phenotype, with either uniformly high or low Pho84 levels (Fig. 4*B*). We interpret these lineages as resulting from seeding by a single "on" or "off" cell; maintenance of the phenotypic state over multiple cell divisions results in an entire lineage with relatively uniform expression level.
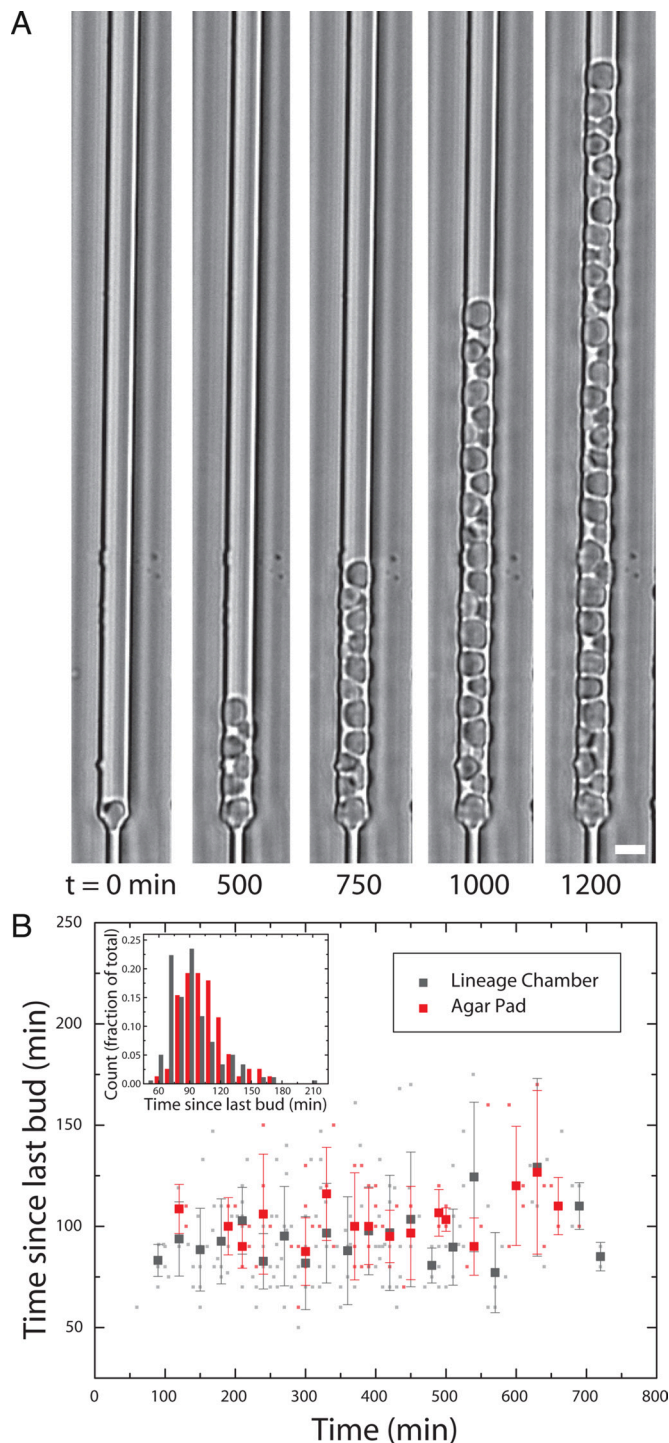
Fig. 3. Cells grow in a line. (*A*) Single progenitor cells are constrained to grow in a line, as shown in this time sequence of bright-field images. (*B*) Doubling times are similar for cells grown in lineage chambers (*n* = 180) versus on agar pads (*n* = 78). Hsp12-GFP cells in YPD media. *Inset*, histogram of doubling times. Bin size, 10 min. (Scale bar, 5 μm.)

We also observe clusters of adjacent cells within a lineage that are either "on" or "off," which result from a change in expression state during lineage growth. We quantify the number of cells per cluster, normalize to the number of cells in the lineage to obtain a "cluster index" (CI), and plot the CI distribution (Fig. 4*C*). When the CI is 1, all cells within an entire lineage have similar protein levels, whereas a CI less than 1 indicates the presence of clusters of cells
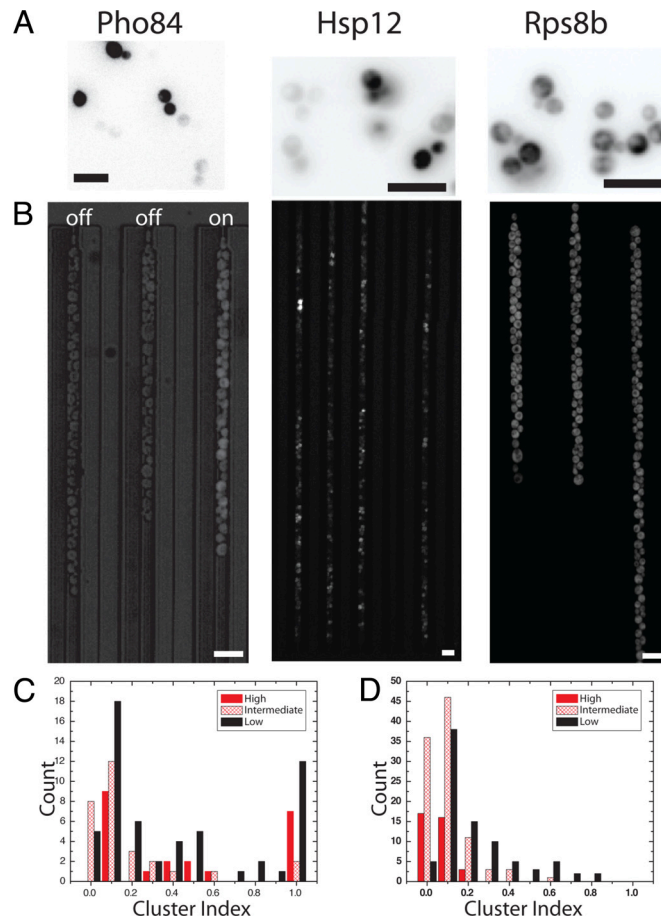
Fig. 4. Phenotypic variation in lineages of cells. Three different proteins, pPho84-GFP, Hsp12-GFP, and Rps8b-GFP, as seen by inverted GFP-fluorescence images (*A*) and after growth in lineage chambers (*B*). We observe lines of high- or low-expressing pPHO84-GFP cells in intermediate phosphate concentration (200 μM phosphate), suggesting that a particular phenotypic state is maintained over multiple divisions. By contrast, the heat shock protein Hsp12-GFP shows smaller clusters, indicating that protein levels change on a relatively faster time scale. Cells that express the ribosomal protein Rps8b-GFP show little variation along lineages. Images are sequentially thresholded to identify cells with similarly high, intermediate, or low fluorescence. The cluster index (CI) is the number of adjacent cells with similar fluorescence divided by the total number of cells in a lineage, and provides a qualitative measure of the number of generations that protein levels persist. CI distributions for *n* individual cells for (*C*) pPHO84-GFP (*n* = 1,309 from 38 tracks); (*D*) Hsp12-GFP (*n* = 1,122 from 33 tracks). (Scale bar, 10 μm.)

that each have a distinct phenotype. Importantly, we observe that clusters form at all positions along the chambers, and that expressing cells may be adjacent to or upstream from non-expressing cells; if cell-cell communication by soluble factors determined protein expression patterns, cells downstream from or adjacent to expressing cells would consistently exhibit similar protein levels. This very simple experiment thus shows that we can detect the persistence of a particular phenotypic state over multiple generations, and thereby demonstrates the efficacy of our system for the study of cell lineages.

We next investigate the behavior of 2 representative proteins that show unimodal bulk distributions, but with different variances: the heat shock protein Hsp12 belongs to a family of stress proteins that exhibit large variation in expression levels compared with essential "housekeeping" proteins such as the ribosomal protein Rps8b (Fig. S3) (13, 14). Indeed, imaging the Hsp12-GFP cells in bulk at a single time point shows that some cells are very bright whereas others express low levels of protein (Fig. 4*A*); however, it is not known how expression levels fluctuate over time. Growing Hsp12-GFP cells in

Rowat et al.

A Rps8b

(Figure 5A: lineage map for Rps8b-GFP, Time (minutes) axis 100–700)

B Hsp12

(Figure 5B: lineage map for Hsp12-GFP, Time (minutes) axis 100–800)

Fluorescence/Mean

Fig. 5. Tracking single cells and their progeny. Dynamic lineage maps of (*A*) Rps8b-GFP and (*B*) Hsp12-GFP. Protein levels are normalized to the mean fluorescence of the population. The genealogical identity of each cell is labeled in the bright-field image (*Right*) acquired at the endpoint. Bursts in Hsp12-GFP protein levels are observed; of the 14 bursts observed here, 8 occur concomitantly in mother-daughter pairs, for example in cells 1 and 15 at 650 min.

the lineage chambers reveals clusters of bright and dark cells within lineages deriving from single cells (Fig. 4*B*). In contrast to pPho84-GFP, clusters of Hsp12-GFP cells with similar expression levels are typically 2 to 6 cells long and we observe no full lineages of cells with similar phenotype (CI < 1), indicating that their phenotypic state varies on a faster generational time scale (Fig. 4*D*). By contrast, lineages of cells expressing Rps8b-GFP show little variation (Fig. 4

A and *B*): all cells within a single lineage have similar protein levels (CI = 1.0). These results demonstrate the ability of our method to distinguish expression patterns across multiple generations of cells among different proteins.

To follow fluctuations in protein levels over time and create a quantitative lineage map, we operate the device in kinetic mode; to accomplish this we acquire images at 10-min intervals and track the cells as they divide using a semiautomated MATLAB program. Each vertical line in the lineage map denotes the appearance of a new progeny cell after division; the complete map thus provides knowledge of each cell's pedigree and replicative age. To reveal variations in protein levels among single cells and their kin, we plot the fluorescence intensity or protein level per cell as a function of time on the lineage map. The ribosomal subunit protein Rps8b-GFP shows relatively constant levels over 8 divisions (Fig. 5*A*). These observations are consistent with hypotheses that cells tightly regulate the expression of housekeeping proteins with essential functions (13, 14). In contrast, levels of Hsp12-GFP fluctuate over time, exhibiting up to 2.5 times as many changes compared with the population mean (Fig. 5*B*). We observe bursts in expression even under steady-state conditions at room temperature, with no applied heat shock. The lineage map reveals that bursts in protein levels appear to be random and do not correlate with extrinsic factors such as cell volume, cell cycle stage, or replicative age. Neither do these fluctuations appear to be attributed to low protein copy number per cell: whereas Rps8b has 1.4×10^4 molecules per cell and Hsp12 has 4.5×10^3 molecules per cell (12), we observe similar fluctuations in the protein Hxk1-GFP, with 4.8×10^4 molecules per cell (data not shown). Interestingly, we observe 57% of bursts occur simultaneously in mother and daughter cells ($n = 48$ cell pairs); the probability that these observations are caused by random fluctuations is very low (χ^2 test, $P \ll 0.001$; *SI Text*). The similar behavior among closely related cells may be attributed to mRNA transferred between mother and daughter that decays on time scales comparable to division times (29) and/or a chromatin configuration that is passed on to progeny at cell division. Similar behavior is observed in yeast cells with an engineered regulation pathway: cells share a similar expression state to their mother cell, as well as the tendency to switch between 2 semi-stable states (5). It is notable that our observations are in a naturally regulated pathway, suggesting that genealogically shared protein expression patterns may be a widespread phenomenon in eukaryotic protein expression.

Non-periodic bursts in expression are predicted from mathematical models of transcription together with stationary distributions obtained by flow cytometry (30) and microscopy (31–33), and are observed in living systems including bacteria (34), during differentiation in Dictyostelium (35), and following DNA damage in mammalian cells (36). Protein levels within a single cell can fluctuate as a result of the stochastic nature of reactions that rely on components present in low copy numbers. These fluctuations may also result from transitions in chromatin packing between inactive and active transcriptional states (32, 37). At the population level, bursting expression generates cell-to-cell variation among genetically identical cells, and suggests that average protein levels could be tuned by changes in the proportion of expressing cells. In the context of evolution, the ability to propagate a particular expression state for several generations could allow for adaptation to environmental change on time scales faster than genetic mutation (2). Although the molecular mechanisms underlying temporal patterns in protein expression in populations of single cells remain to be fully elucidated, the ability to monitor protein levels in single yeast cells and their progeny over many generations is a prerequisite for systematic studies of fluctuations in protein levels over time, as well as in the context of pedigree.

Conclusion

The simple lineage chamber system that we describe here enables studies of fluctuations and patterns in protein expression

that propagate in single cells over time and over multiple generations. In addition, it is possible to study any asymmetries at cell division, correlations between cells caused by their pedigree, replicative age, or any other physical trait such as volume. The pedigree analysis software is generally applicable to any yeast strain, and does not require additional fluorescent markers for progeny identification. A further benefit of our device is the ability to fix and stain single suspension cells and their lineages, allowing morphological phenotypes on subcellular scales to be resolved, for example, by immunofluorescence or FISH. With slight modifications in size, the lineage chambers can also be used for culture of other suspension cells, including mammalian blood cells or stem cells. More broadly, our device will enable studies revealing correlations among single cells and their progeny that remain masked in the ensemble average.

Materials and Methods

Lumped Element Modeling. For a rectangular channel, the relationship between the pressure drop ΔP and flow rate Q is given by the Hagen-Poiseuille relation, $\Delta P = 12Q\eta l/h^3w$, where η is the dynamic viscosity and w, h, and l are the channel width, height, and length. The bypass channel is considered as a single resistor, R_2, with dimensions w_2, h_2, and l_2. The trapping channel consists of 2 resistors: R_{1a}, the long channel with dimensions w_{1a}, h_{1a}, and l_{1a}; and R_{1b}, the narrow constriction neck with dimensions w_{1b}, h_{1b}, and l_{1b} (Fig. 1A). The ratio of flow through the bypass to trapping channel is expressed as follows:

$$\frac{Q_2}{Q_1} = \frac{R_{1a} + R_{1b}}{R_2} = \frac{h_2^3 w_2}{l_2} \left[\frac{l_{1a}}{h_{1a}^3 w_{1a}} + \frac{l_{1b}}{h_{1b}^3 w_{1b}} \right] \quad [1]$$

Microfluidic Device Fabrication. Soft lithography is used to fabricate microfluidic channels in PDMS (Sylgard 184 silicone elastomer; Dow Corning) (38). Devices are bonded to Lab-tek II 2-well chambered cover glass (no.1.5 borosilicate glass; Nalge Nunc no. 62407–052; Thermo Fisher Scientific).

Yeast Cell Culture. Cell strains are from the GFP-library (Invitrogen). The pPHO84-GFP strain (w303, MATa, pPHO84-yeG::URA3) is a generous gift from the lab of Erin O'Shea (Cambridge, MA). Liquid cultures are inoculated from a single colony into yeast extract/peptone/dextrose (YPD) or intermediate phosphate concentration media (39) and are shaken at room temperature for 24 h to a density of 2 to 6×10^5 cells/mL.

Device Operation. Syringe pumps (Harvard Apparatus) control fluid flow. To track flow velocities through the channels, we flow 0.465-μm polystyrene beads (Polysciences) through the device at 5 μL/h and acquire images at 5,000 frames per second with a high-speed camera (Phantom v7.3; Vision Research).

Growth Rates. Agar pads are made by molding 1.5% wt/wt agar in YPD between 2 glass slides separated by a rubber spacer (Grace Bio-Labs; Sigma).

Imaging. We acquire images of cells every 10 min by using an inverted microscope equipped with an automated stage (Prior Scientific), $\times$20 objective, and GFP filter set.

Image Analysis. CI analysis is performed by twice sequentially thresholding the endpoint image to identify adjacent cells with high, intermediate, and low fluorescence. To construct complete lineage maps, we acquire a bright field and fluorescence image at 10-min time intervals and track cells using custom MATLAB software (MathWorks).

1. Raj A, van Oudenaarden A (2008) Nature, nurture, or chance: Stochastic gene expression and its consequences. *Cell* 135:216–226.
2. Rando OJ, Verstrepen KJ (2007) Timescales of genetic and epigenetic inheritance. *Cell* 128:655–668.
3. Novick A, Weiner M (1957) Enzyme induction as an all-or-none phenomenon. *Proc Natl Acad Sci USA* 43:553–566.
4. Acar M, Becskei A, van Oudenaarden A (2005) Enhancement of cellular memory by reducing stochastic transitions. *Nature* 435:228–232.
5. Kaufmann BB, Yang Q, Mettetal JT, van Oudenaarden (2007) A heritable stochastic switching revealed by single-cell genealogy. *PLoS Biol* 5:e239.
6. Li L, Lindquist S (2000) Creating a protein-based element of inheritance. *Science* 287:661–664.
7. Smith CM, et al. (2002) Heritable chromatin structure: mapping ''memory'' in histones H3 and H4. *Proc Natl Acad Sci USA* 99(suppl 4):16454–16461.
8. Kussell E, Leibler S (2005) Phenotypic diversity, population growth, and information in fluctuating environments. *Science* 309:2075–2078.
9. Lachmann M, Jablonka E (1996) The inheritance of phenotypes: An adaptation to fluctuating environments. *J Theor Biol* 181:1–9.
10. Balaban NQ, Merrin J, Chait R, Kowalik L, Leibler S (2004) Bacterial persistence as a phenotypic switch. *Science* 305:1622–1625.
11. Huh WK, et al. (2003) Global analysis of protein localization in budding yeast. *Nature* 425:686–691.
12. Ghaemmaghami S, et al. (2003) Global analysis of protein expression in yeast. *Nature* 425:737–741.
13. Newman JR, et al. (2006) Single-cell proteomic analysis of S. cerevisiae reveals the architecture of biological noise. *Nature* 441:840–846.
14. Bar-Even A, et al. (2006) Noise in protein expression scales with natural protein abundance. *Nat Genet* 38:636–643.
15. Murray AW, Szostak JW (1983) Pedigree analysis of plasmid segregation in yeast. *Cell* 34:961–970.
16. Groisman A, et al. (2005) A microfluidic chemostat for experiments with bacterial and yeast cells. *Nat Methods* 2:685–689.
17. Cookson S, Ostroff N, Pang WL, Volfson D, Hasty J (2005) Monitoring dynamics of single-cell gene expression over multiple cell cycles. *Mol Syst Biol* 1:2005 0024.
18. Balagadde FK, You L, Hansen CL, Arnold FH, Quake SR (2005) Long-term monitoring of bacteria undergoing programmed population control in a microchemostat. *Science* 309:137–140.
19. Paliwal S, et al. (2007) MAPK-mediated bimodal gene expression and adaptive gradient sensing in yeast. *Nature* 446:46–51.
20. Lee PJ, Helman NC, Lim WA, Hung PJ (2008) A microfluidic system for dynamic yeast cell imaging. *Biotechniques* 44:91–95.
21. Charvin G, Cross FR, Siggia ED (2008) A microfluidic device for temporally controlled gene expression and long-term fluorescent imaging in unperturbed dividing yeast cells. *PLoS ONE* 3:e1468.
22. Di Carlo D, Wu LY, Lee LP (2006) Dynamic single cell culture array. *Lab Chip* 6:1445–1449.
23. Luo C, et al. (2008) A fast cell loading and high-throughput microfluidic system for long-term cell culture in zero-flow environments. *Biotechnol Bioeng* 101:190–195.
24. Ryley J, Pereira-Smith OM (2006) Microfluidics device for single cell gene expression analysis in Saccharomyces cerevisiae. *Yeast* 23:1065–1073.
25. Davis RH, Perkins DD (2002) Timeline: Neurospora: A model of model microbes. *Nat Rev Genet* 3:397–403.
26. Tan WH, Takeuchi S (2007) A trap-and-release integrated microfluidic system for dynamic microarray applications. *Proc Natl Acad Sci USA* 104:1146–1151.
27. Yen RT, Fung YC (1978) Effect of velocity of distribution on red cell distribution in capillary blood vessels. *Am J Physiol* 235:H251–H257.
28. Wykoff DD, Rizvi AH, Raser JM, Margolin B, O'Shea EK (2007) Positive feedback regulates switching of phosphate transporters in S. cerevisiae. *Mol Cell* 27:1005–1013.
29. Wang Y, et al. (2002) Precision and functional specificity in mRNA decay. *Proc Natl Acad Sci USA* 99:5860–5865.
30. Friedman N, Cai L, Xie XS (2006) Linking stochastic dynamics to population distribution: an analytical framework of gene expression. *Phys Rev Lett* 97:168302.
31. Newlands S, et al. (1998) Transcription occurs in pulses in muscle fibers. *Genes Dev* 12:2748–2758.
32. Raj A, Peskin CS, Tranchina D, Vargas DY, Tyagi S (2006) Stochastic mRNA synthesis in mammalian cells. *PLoS Biol* 4:e309.
33. Zenklusen D, Larson DR, Singer RH (2008) Single-RNA counting reveals alternative modes of gene expression in yeast. *Nat Struct Mol Biol* 15:1263–1271.
34. Cai L, Friedman N, Xie XS (2006) Stochastic protein expression in individual cells at the single molecule level. *Nature* 440:358–362.
35. Chubb JR, Trcek T, Shenoy SM, Singer RH (2006) Transcriptional pulsing of a developmental gene. *Curr Biol* 16:1018–1025.
36. Lahav G, et al. (2004) Dynamics of the p53-Mdm2 feedback loop in individual cells. *Nat Genet* 36:147–150.
37. Raser JM, O'Shea EK (2004) Control of stochasticity in eukaryotic gene expression. *Science* 304:1811–1814.
38. Duffy DC, McDonald JC, Schueller OJA, Whitesides GM (1998) Rapid prototyping of microfluidic systems in poly(dimethylsiloxane). *Anal Chem* 70:4974–4984.
39. Huang S, Jeffery DA, Anthony MD, O'Shea EK (2001) Functional analysis of the cyclin-dependent kinase inhibitor Pho81 identifies a novel inhibitory domain. *Mol Cell Biol* 21:6695–6705.